Phys. Status Solidi RRL **5**, No. 5–6, 199–201 (2011) / **DOI** 10.1002/pssr.201105183

pss +++rapid research letters+++
www.pss-rapid.com

# Detecting efficiency-limiting defects in Czochralski-grown silicon wafers in solar cell production using photoluminescence imaging

**Jonas Haunschild*, Isolde E. Reis, Juliane Geilker, and Stefan Rein**

Fraunhofer Institute for Solar Energy Systems ISE, Heidenhofstr. 2, 79110 Freiburg, Germany

Received 8 April 2011, revised 26 April 2011, accepted 2 May 2011
Published online 5 May 2011

**Keywords** Czochralski silicon, photoluminescence imaging, oxygen precipitates, solar cells

* Corresponding author: e-mail Jonas.Haunschild@ise.fraunhofer.de, Phone: +49 761 4588 5563, Fax: +49 761 4588 9250

Only recently, methods for quality control of multicrystalline silicon wafers have been published, which allow the efficiency of solar cells to be predicted precisely from photoluminescence (PL) images taken in the as-cut state. In this letter it is shown that oxygen precipitates, present in standard Czochralski silicon wafers, can cause efficiency losses of more than 4% (absolute) within an industrial solar cell process. These efficiency losses correlate with ring-like defect structures of reduced intensity in the PL image. In comparison with QSSPC-based lifetime measurements, we introduce a PL-based method of quality control which allows the critical wafers to be identified and sorted out reliably at an early state of production and thus increases yield and average efficiency of production lines.



**1 Introduction** Six years after the first paper on electroluminescence imaging was published by Fuyuki et al. [1], this technique has become an important characterization tool for solar cell production lines. An overview on the methods and fields of application of luminescence imaging can be found in [2].

One of the most promising applications for contactless photoluminescence (PL) imaging is quality control of multicrystalline silicon (mc-Si) wafers in the as-cut state. Special features from single PL images can be extracted via image processing and can be attributed to specific material defects. Knowing their impact on solar cell efficiency, a precise quality control is realized [2, 3].

Recently ring-like patterns have been observed in PL images of Czochralski (Cz)-Si wafers [4, 5], therefore we investigate the material quality of a variety of commercially available Cz-Si wafers from different manufacturers and the resulting limitations of solar cell efficiency in an industrial solar cell process based on screen-printing. In a second step, we evaluate different techniques available for inline process control with respect to their capability to detect the observed defects. Note that throughout this paper material quality is not investigated with respect to the metastable bond-order (BO) defect responsible for lifetime degradation [6], but with respect to other more severe background defects.

**2 Solar cell characterization** For this study, Cz-Si wafers from different manufacturers which entered the PV-TEC production line at Fraunhofer ISE over a time span of several years were randomly selected and characterized with PL imaging. From these random samples a batch of 156 × 156 mm$^2$ solar cells was manufactured using a standard industrial solar cell process based on screen-printing. The finished solar cells were then IV tested (in

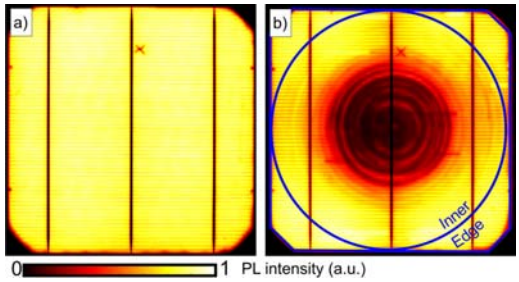


**Figure 1** (online colour at: www.pss-rapid.com) PL images of solar cells with (a) 18.4% and (b) 14.4% efficiency. The marked areas are used for evaluation of the ring defect.

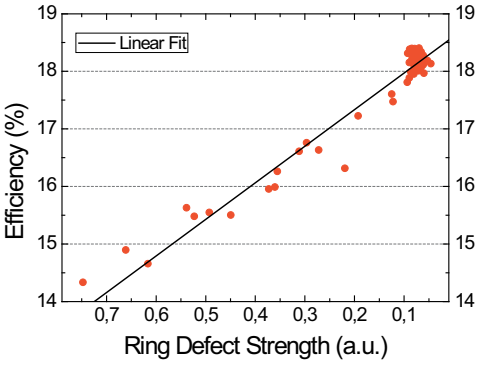


**Figure 2** (online colour at: www.pss-rapid.com) Solar cell efficiency as a function of the ring defect strength (defined as ratio of the average PL intensities in the centre and the edge region displayed in Fig. 1) measured at the finished Cz-Si solar cells. A linear correlation of both quantities is found on a statistical base of 81 samples.

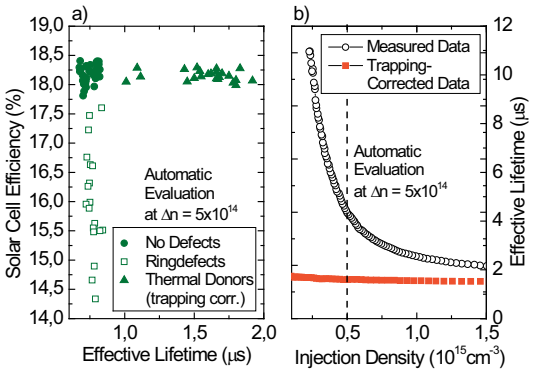


**Figure 3** (online colour at: www.pss-rapid.com) (a) Solar cell efficiency as a function of effective carrier lifetime, measured by means of QSSPC on the as-cut wafers. (b) Underlying injection-dependent lifetime curve. Lifetime is limited by surface recombination and superimposed by charge carrier trapping which may be corrected.

the non-degraded state). Solar cells whose efficiency was limited by process-induced defects such as shunts or high series resistances have been identified by applying thermographical measurements and quantitative PL imaging [7] and were excluded from this study to focus only on material-related issues.

In Fig. 1, PL images of solar cells with efficiencies of 14.4% and 18.4%, respectively, are shown. As process-related problems can be excluded, efficiency is limited by the ring-like defect structure, which is highly recombination-active and thus appears dark in the PL image in Fig. 1b. The observed efficiency drop by 4% (absolute) can thus be attributed to poor material quality. In Fig. 2 solar cell efficiency is plotted against the strength of the ring defect for the whole batch of 81 samples. The ring defect strength was defined as the ratio of the mean count rates of the luminescence signal in the inner area and the outer edge areas of the solar cell (marked in Fig. 1) under open circuit conditions. The position of the circle was chosen to cover the largest extension of rings in this study and is applied to all solar cells. The correlation found by this very simple approach clearly shows that the ring defect is responsible for the reduced efficiencies. If rings cover the whole area this approach might fail.

**3 As-cut characterization** It would be desirable to identify wafers with too low material quality during incoming inspection to be able to directly reject these wafers or to transfer them to specially adjusted production lines. In Fig. 3a, solar cell efficiency is plotted as a function of the effective charge carrier lifetime measured on the individual wafers in the as-cut state using the quasi-steady state photoconductance (QSSPC) technique. With the inline-setup used, the measurement is performed in a circular area of 80 mm diameter in the center of the wafer and the lifetime values are extracted at an injection density $\Delta n = 5 \times 10^{14}$ cm$^{-3}$. The data can be classified in three groups which are distinguished in the graph by different symbols. The first group of wafers with high as-cut lifetimes above 1.0 µs (triangles) did not result in higher efficiencies. The injection-dependent lifetime curve in Fig. 3b shows that these lifetime values are partially increased by trapping artifacts which cannot be completely removed in spite of a trapping correction according to Ref. [8]. As the observed lifetime increase towards low-injection densities disappeared upon annealing in conjunction with a decrease of base resistance, it can be attributed to thermal donors. For the second group of wafers with as-cut lifetimes in the range of 0.7 µs (circles) the small differences in carrier lifetime do not correlate to small differences in cell efficiency. In this case the lifetime in the finished cell obviously is high enough to reach the efficiency limit of the process. However, for the third group of wafers with as-cut lifetimes in the same range (open squares) cell efficiency varies strongly from 14.4% to 17.6%, which is not reflected in lifetime in the as-cut state. This behavior is caused either by the surface limitation of carrier lifetime or by a defect activation at a later process stage.

In PL imaging, all wafers from Fig. 2 which resulted in reduced efficiencies already showed ring-like defect structures in the as-cut wafers. Unfortunately, thermal donors

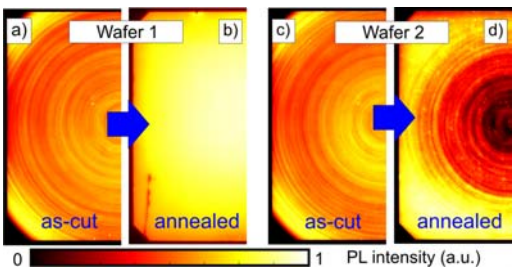


**Figure 4** (online colour at: www.pss-rapid.com) Comparison of PL images measured on two wafers in the as-cut state (a and c) and after an annealing step (b and d). While the ring-like pattern in the PL images of the as-cut wafers looks similar, it vanishes for wafer 1 (b) and becomes stronger for wafer 2 (d) after an annealing step.

can form similar features in the PL image. Figure 4 shows the PL images of two wafers from group 1 and 3 measured before and after an annealing step for 10 s at 800 °C. As can be seen from Fig. 4a and b, in a wafer with thermal donors (group 1), the ring-structures vanish completely after annealing and thus do not influence cell efficiency. Figure 4c and d show that group 3 wafers show similar PL images in the as-cut state as the group 1 wafers. But as can be seen in Fig. 4d, the ring-like defect structure in this wafer does not vanish upon annealing but becomes much stronger and thus results in a lower cell efficiency. Thus, efficiency limiting defects in Cz-Si wafers cannot be separated from thermal donors in the as-cut state so far.

**4 Characterization after emitter diffusion** In production, thermal donors are dissolved during rapid cooling after high temperature steps, so precise quality control should be possible after emitter diffusion. Figure 5 shows the solar cell efficiencies plotted as a function of the (a) effective lifetime obtained from inline QSSPC and (b) the ring defect strength extracted from PL images, both quantities measured after emitter diffusion. While low efficiencies can obviously be attributed to low carrier lifetimes, the solar cell process limits cell efficiency above approx. 20 µs. The PL ring defect strength evaluation yields similar results and confirms that the low lifetimes originate from ring features. Therefore, both methods can be used for a wafer rating after emitter diffusion.

**5 Oxygen precipitates** Figure 6 shows images of the two wafers from Fig. 4 which have been taken by an optical microscope after emitter diffusion. The surface of these wafers has been polished and then preferentially etched [9]. The dots represent oxygen precipitates which may be responsible for the reduced efficiency. The low efficiency wafer from group 3 has a higher density of precipitates than the wafer from group 1 with high efficiency. Using infrared spectroscopy (FTIR) the interstitial oxygen content has been determined to $10^{17}$ cm$^{-3}$ (wafer from group 3, with ring defects after diffusion) and $7 \times 10^{17}$ cm$^{-3}$

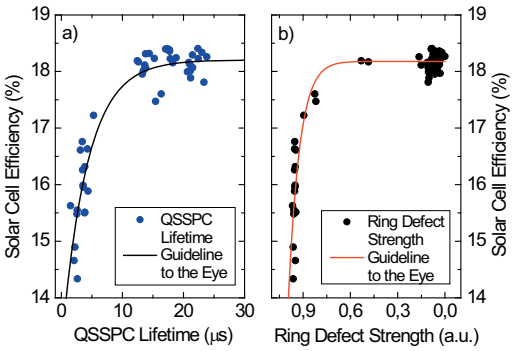


**Figure 5** (online colour at: www.pss-rapid.com) Solar cell efficiency plotted against QSSPC lifetime and PL ring defect strength, respectively, both measured after emitter diffusion. With both methods wafers resulting in low efficiency can be identified reliably.

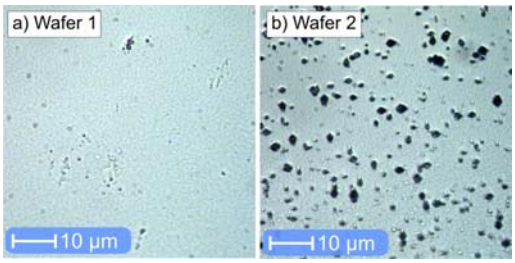


**Figure 6** (online colour at: www.pss-rapid.com) Optical microscope images of wafers taken after polishing and preferential etching. (a) Wafer 1 without ring defects after diffusion shows no oxygen precipitates. (b) Wafer 2 with strong ring defects after diffusion shows lots of oxygen precipitates.

(wafer from group 1, without ring defects after diffusion). Oxygen-related defects have been characterized thoroughly for semiconductor devices [10]. Depending on the pulling speed during crystallization, interstitial- or vacancy-rich regions can form which assist precipitation differently. The variety of these defects is large and the influence on carrier lifetime varies. Some can be activated by high-temperature steps and some are deactivated, depending on temperature and slope of temperature change. A detailed analysis of the defects being present in the wafers of this study has to be performed and requires complex sample preparation and high temperature annealing steps at different temperatures and slopes, which is beyond the scope of this paper.

**6 Conclusion** In this study it could be shown that defects which reduce solar cell efficiency by more than 4% (absolute) are present in commercially available Cz-Si materials labelled to be “high quality”. Detection of these defects in the as-cut state during incoming inspection is possible using PL imaging if the presence of thermal donors can be excluded. As this is often not the case, reliable quality control is only possible after emitter diffusion using QSSPC lifetime measurements and PL imaging, respectively.

**Acknowledgement** This work has been supported by the Fraunhofer Society under the frame of the project ABICS-LUM.

## References

[1] T. Fuyuki et al., Appl. Phys. Lett. **86**, 262108 (2005).
[2] T. Trupke et al., Phys. Status Solidi RRL **5**, 131 (2011).
[3] W. McMillan et al., in: Proc. 25th EU-PVSEC Valencia, Spain, 1346 (2010).
[4] A. Lawerenz et al., in: Proc. 25th EU-PVSEC Valencia, Spain, 2486 (2010).
[5] P. J. Cousins et al., in: Proc. 35th IEEE-PVSC Hawaii, USA, 000275 (2010).
[6] B. Lim et al., J. Appl. Phys. **107**, 123707 (2010).
[7] M. Glatthaar et al., Phys. Status Solidi RRL **4**, 13 (2010).
[8] R. Sinton et al., in: Proc. 25th EU-PVSEC Valencia, Spain, 1073 (2010).
[9] E. Sirtl et al., Z. Met.kd. **52**, 529 (1961).
[10] V. V. Voronkov et al., J. Electrochem. Soc. **149**, G167 (2002).